1/3/2024

Internship Report

Prepared for

Archana Rajput

Assistant Professor

IIT Jammu

By

Deepak Kumar
NIT Agartala

Debajyoti Roy
NIT Agartala

Wideband Meta Surface-Based Reflective Polarization Converter for Linear-to-Linear and Linear-to-Circular Polarization Conversion

Software used: CST STUDIO SUITE

Introduction: Wideband generally refers to a system or signal that has a broad frequency range. This term is mainly used in telecommunication and radio frequency (RF) engineering.

A meta surface is a two-dimensional arrangement of subwavelength structures (the individual elements on a meta surface are designed to be smaller than the wavelength of incident electromagnetic waves) mainly designed to control and manipulate the electromagnetic waves. A meta surface structure split ring resonator has been employed to achieve wideband polarization conversion in this case.

Polarization refers to the orientation of electric field in an electromagnetic wave while the polarization converter is a device or material that transforms the polarization state of electromagnetic wave. If we examine a y polarized electromagnetic wave, it is transformed to x polarization for linear-to-linear polarization conversion and vice versa. Also, the same wave can be converted into CP reflected wave for Linear-to-circular polarization.

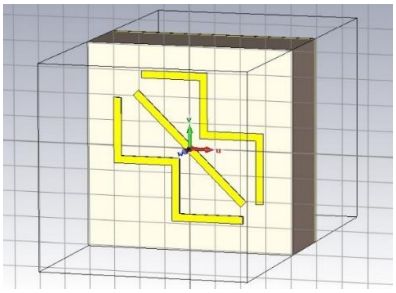

Fig 1: Schematic of the unit cell.

Design and Analysis of the Meta surface

Configuration of unit cell:

The schematic of the unit cell of the proposed polarization converter is shown in fig 1. The structure comprised of three parts:

1) A top metallic copper structure (An I-shaped structure that converts a linearly polarized incident wave to a circularly polarized reflection wave and a Double L-shaped meta surface that converts an LP incident wave to a CP reflected wave were also introduced to create a multipolarization converter.) The top metallic structure comprises of

(a) Two symmetric meander lines

(b) A cut-wire structure which is placed -45° along +y axis.

2) With a dielectric constant of 4.4 and a dielectric loss tangent of 0.02 the FR-4 is an intermediate dielectric substrate.

3) A metallic copper ground plate at the bottom that is 0.035 mm thick and has a conductivity of 5.8 x 10^7 S/m.

With the floquet port pointing in the +z direction and the master/slave borders pointing in the x and y directions, the unit cell is simulated.

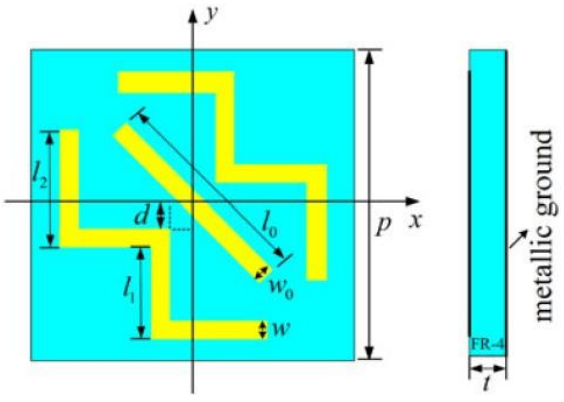

Parameters	Dimensions
p	8.1mm
t	3.1mm
d	0.4mm
L1	2.5mm
w, wo	0.3mm
L2	2.3mm
Lo	6mm

S parameters: S-parameters describe the input-output relationship between ports (or terminals) in an electrical system. For instance, if we have 2 ports (intelligently called Port 1 and Port 2), then S12 represents the power transferred from Port 2 to Port 1. S21 represents the power transferred from Port 1 to Port 2. In general, SNM represents the power transferred from Port M to Port N in a multi-port network.

In practice, the most quoted parameter regarding antennas is S11. S11 represents how much power is reflected from the antenna, and hence is known as the reflection coefficient.

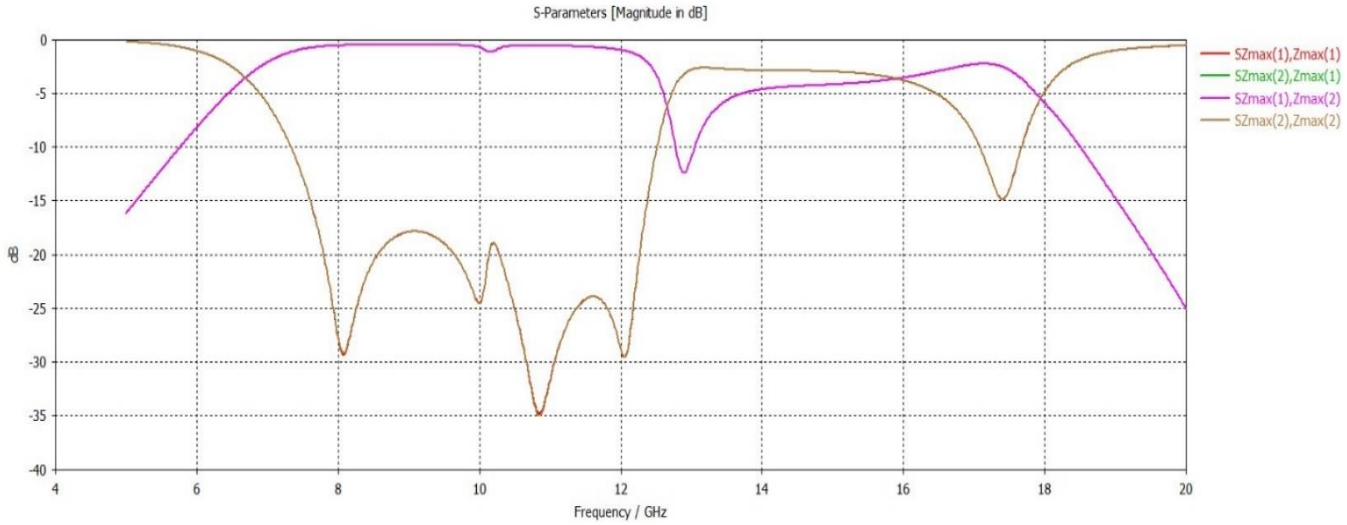

Fig:2(a) Co and cross-polarized reflection coefficients.

Fig 2(a) illustrates the co and cross polarization characteristics. The co-polarization remains below -9dB in the frequency range of 7.2 to 12.5 GHz. Additionally, from 15.3 to 16.2 GHz, the co and cross polarization exhibit nearly equal values.

In co-polarization, the transmitted and received waves have the same polarization state. For example, if the transmitted wave is horizontally polarized (H), the received wave is also horizontally polarized.

In cross-polarization, the transmitted and received waves have orthogonal polarization states. For example, if the transmitted wave is horizontally polarized (H), the received wave is vertically polarized (V).

Using a y-polarized incident wave as an example, we define

rxy=$|E_x^r/E_y^i|$ and ryy=$|E_y^r/E_y^i|$ to represent the cross polarization (y to x) and co-polarization(y to y) respectively.

PCR(Polarization Conversion Ratio):The term “polarization conversion ratio” typically refers to the efficiency or effectiveness of a device or process in converting the polarization state of light .

$$PCR = rxy^2 / (rxy^2 + ryy^2)$$

ECR(Energy Conversion Ratio):The ratio of energy conversion ECR is used to calculate overall energy conversion efficiency.

$$ECR = (rxy^2 + ryy^2)$$

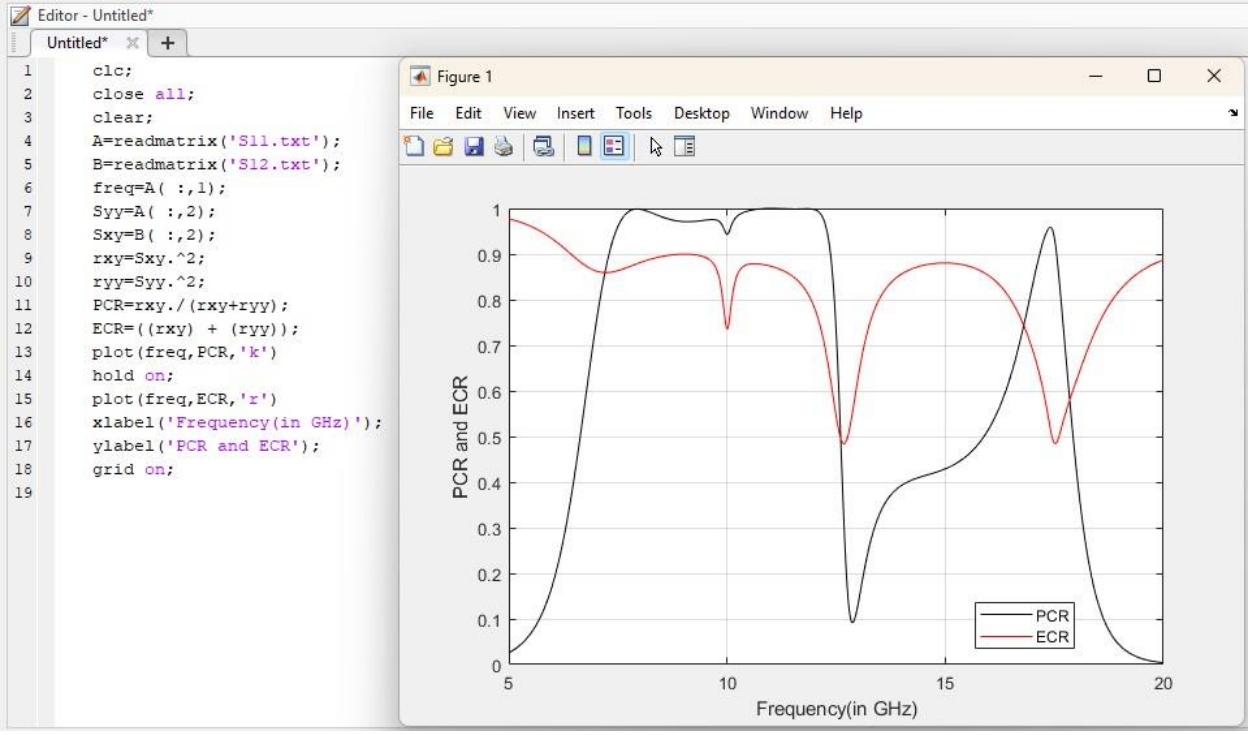

Fig:2(b) PCR and ECR vs Frequency

In the frequency range of 7 to 12.3 GHz, it is observed that the polarization conversion ratio(PCR) exceeds 0.88. This observation suggests that the incident Linearly polarized(LP) wave undergoes efficient rotation to its orthogonally reflected LP wave with a high degree of Polarization conversion efficiency. Notably, two resonance frequencies are identified at 7.91 and 11.95 GHz.

The Polarization Cross-Reflection (PCR) is 0.5 ± 0.05 within the frequency range of 14.7 to 15.62 GHz, with the point of 0.5 PCR specifically at 15.89 GHz. This indicates that approximately half of the energy is redirected into its orthogonal direction.

Figure 2(b) illustrates that the Circular Polarization (CP) efficiency remains above 0.89 across the frequency range of 14.7 to 15.62 GHz. These findings indicate that the suggested structure demonstrates a high-efficiency conversion characteristic.

Axial Ratio:

In the following step, we use azimuth angle ($\eta = \arctan(|E_{rx}|/|E_{ry}|)$, [0°, 90°]) and the axial ratio (AR) (dB, As illustrated in Fig. 3, the phase difference between the entire reflected field along the x- and y-axes ($\Delta\phi_{xy} = \phi_x - \phi_y$, [180°, 180°]) is presented to analyze precise circular polarization states. When $\eta = 90°$, the reflection is an ideal linear polarization (AR =), and when $\eta = 45°$ and $\Delta\phi_{xy} = \pm 45°$, the reflection is a perfect circular polarization (AR = 0). The remainder are elliptical polarization. We use a 3 dB AR bandwidth in this letter to analyze its circular-polarization characteristic.

The azimuth angles at 7.985 and 11.975 GHz are 87.0142° and 87.5017°, respectively, as shown in Fig. 3(a), indicating that the reflected waves are linear polarization. At 15.905 GHz, the azimuth angle equals 45°, indicating that the magnitudes of the reflected field's x- and y-components

are equal. It also denotes a possible candidate for circular polarization. As shown in Fig. 3(b), the AR values are greater than 39 dB at two resonance frequencies (7.985 and 11.975 GHz), indicating that the reflection waves have linear polarizations. . It can be shown that from 14.255 to 16.235 GHz, 3dB AR bandwidth is acquired. The phase difference shown in fig 3(d) meets $\Delta\phi_{xy}$ =-90˚.As a result, the reflected wave has a circular polarization.

$$AR = \sqrt{\frac{|r_{yy}|^2 + |r_{xy}|^2 + \sqrt{|r_{yy}|^4 + |r_{xy}|^4 + 2|r_{yy}|^2|r_{xy}|^2\cos(2\Delta\varphi_{yx})}}{|r_{yy}|^2 + |r_{xy}|^2 - \sqrt{|r_{yy}|^4 + |r_{xy}|^4 + 2|r_{yy}|^2|r_{xy}|^2\cos(2\Delta\varphi_{yx})}}}$$

```
clc;
clear ;
A=readmatrix('LS12.txt');
B=readmatrix('LS22.txt');
freq=A( :,1);
txy=A( :,2);
tyy=B( :,2);
et=atan(txy./tyy);
ett=(et*180)./pi;

plot(freq,ett,'k')
xlabel('Frequency(in GHz)');
ylabel('Azimuthal Angle eta');
grid on;
```

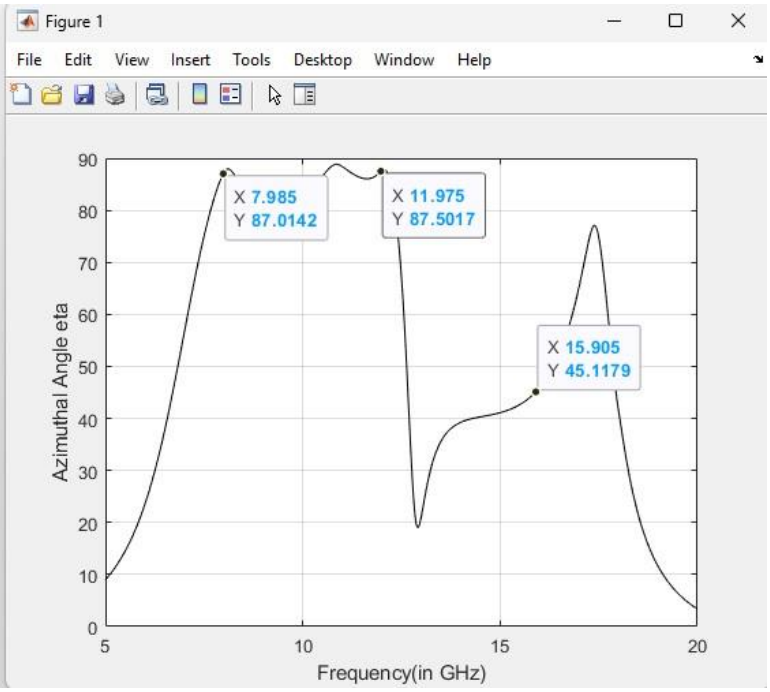

Fig 3(a): Azimuthal angle (η) vs Frequency

```
clc;
clear ;
A=readmatrix('AR_S11.txt');
B=readmatrix('AR_S12.txt');
freq=A( :,1);
txx=A( :,2);
tyy=B( :,2);
deltaphixy=45;
a=(txx.^4)+(tyy.^4)+(2.*(txx.^2).*(tyy.^2).*cos(2.*deltaphixy));
x=(txx.^2)+(tyy.^2)+sqrt(a);
y=(txx.^2)+(tyy.^2)-sqrt(a);
q=x/y;
AR1=sqrt(q);
AR=20*log(AR1);
plot(freq,AR,'k');
grid on;
xlabel('Frequency(GHz)');
ylabel('Axial Ratio(dB)');
title('Axial Ratio vs Frequency');
```

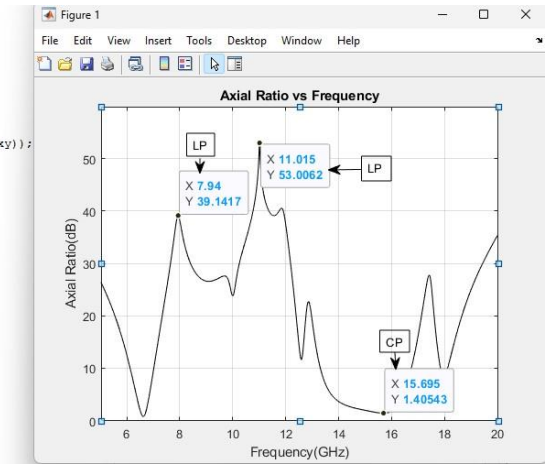

Fig 3(b): AR versus Frequency

```
clc;
A=readmatrix("12deg.txt");
B=readmatrix("22deg.txt");
freq=A(:,1);
Syy=A( :,2);
Sxy=B( :,2);
phi=(Syy-Sxy);
plot(freq,phi,'b');
ylim([-200,300]);
grid on;
ylabel('Relative phase(deg)');
xlabel('frequency(GHz)');
title('Phase difference vs Frequency')
```

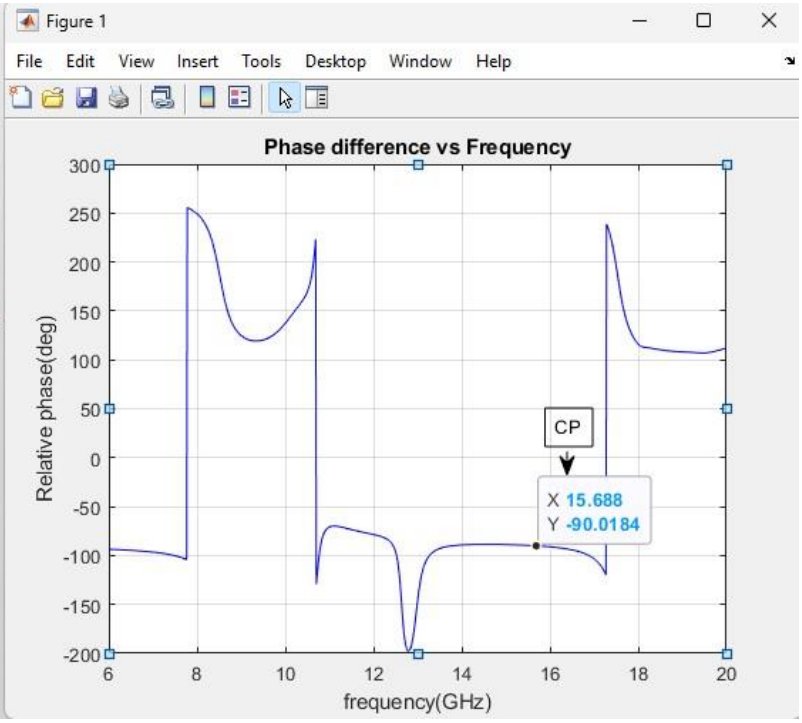

Fig 3(c): Detailed phase difference

B. Analysis of Polarization Conversion:

The polarization converter's unit cell is crafted with an anisotropic structure, derived from a cut-wire resonator. To delve into the polarization converter's mechanisms, an anisotropic coordinate system (u-v axis) is established. In this system, the u- and v-axes are oriented at ±45 ° along

the +y direction, as illustrated in Fig. 4(a). For instance, when a linearly polarized incident wave propagates along the +y-axis, it undergoes decomposition into two equal components.

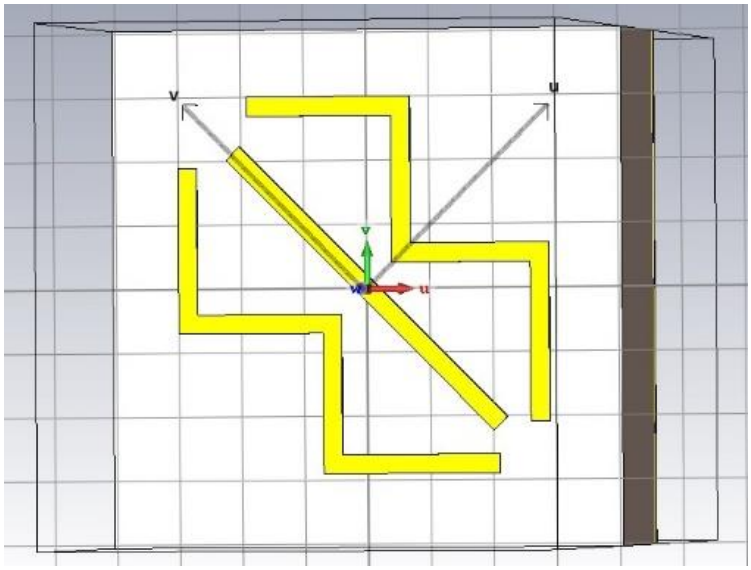

Fig 4(a): New Coordinate system u-v axis

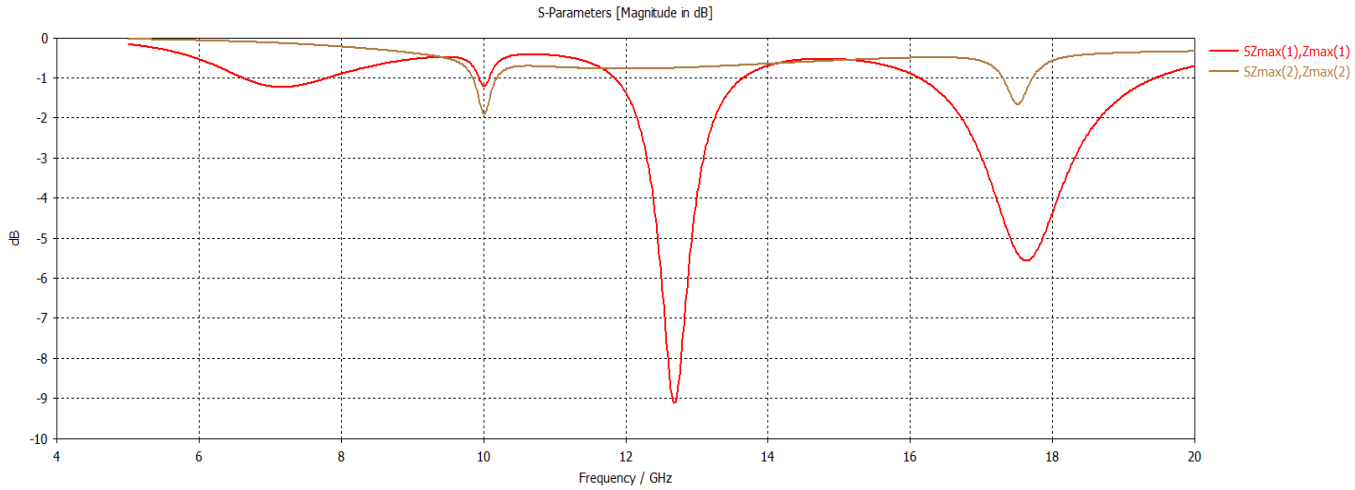

Fig 4(b): Reflection magnitudes

```
A=readmatrix('ps11.txt');
B=readmatrix('ps22.txt');
freq=A( :,1);
txy=A( :,2);
tyy=B( :,2);
P=txy-tyy
plot(freq,P)
grid on;
xlabel('Frequency(GHz)');
ylabel('Phase Difference');
title('Phase Difference vs Frequency');
```

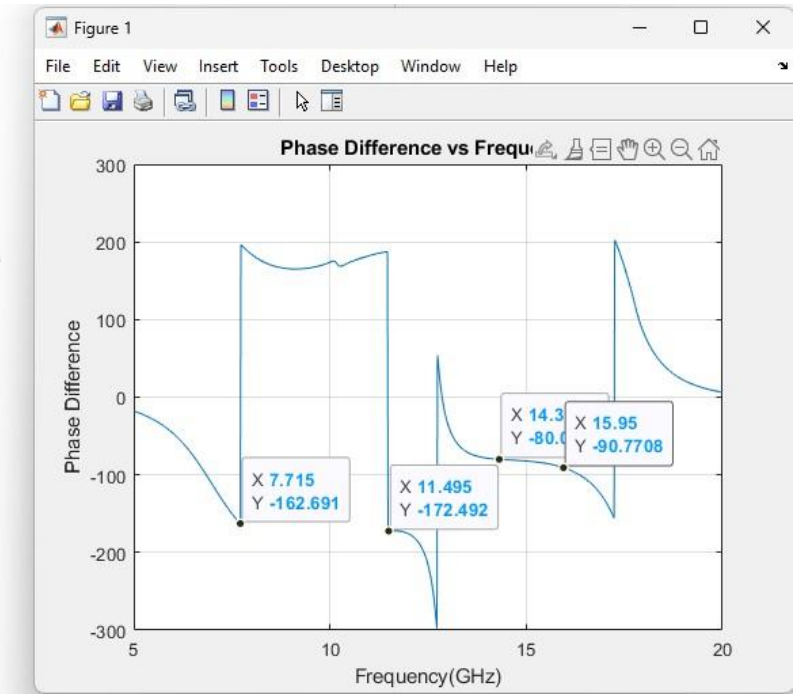

Fig 4(c): Reflection phases under u- and v-polarization and the phase difference

In Figure 4(b) and (c), the reflection magnitudes, phases under u- and v-polarized directions (ϕu and ϕv), and the phase difference (Δϕuv = |ϕu − ϕv|) are presented. It is evident that the discrepancies in reflected magnitudes along the uv-axis are below 0.1 within the frequency bands of 8.75–9.8 GHz and 13.5–15.75 GHz. Specifically, the reflection phase differences exhibit a pattern of approximately 180 ˚ from 7.715 to 11.495 GHz and around 90 ˚ from 14.3 to 15.95 GHz. These findings suggest that the proposed structure shows promise in converting the linearly polarized electromagnetic wave into linearly polarized and circularly polarized reflection waves in lower and higher frequency bands, respectively.

There are three basic steps in the design procedure:

Part I consists of designing two symmetric meander lines.

Part II is designing a single cut-wire resonator.

Part III is optimizing the parameters.

Obtaining a wideband high PCR is the primary goal of the first stage, since it guarantees that the LP incident wave may be turned to its orthogonal LP reflection. The purpose of the cut-wire resonator, which is around 0.6 times longer than the meander-line resonator that was first proposed, is to generate a circular polarization in the higher band by disrupting polarization states. Ultimately, the optimization of the structure is achieved to produce both a CP reflection wave in the higher band and an LP reflection wave in the lower band.

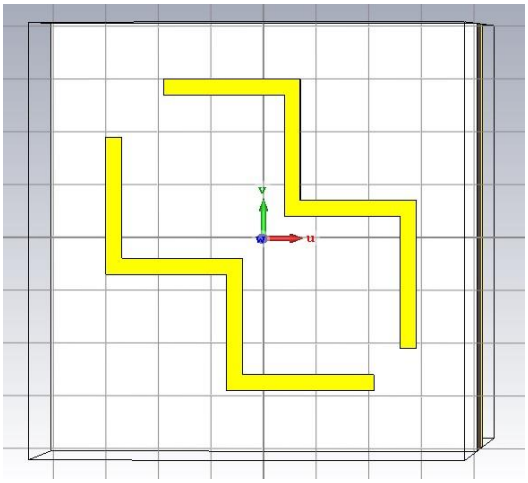

Fig: Part 1(Meander Lines)

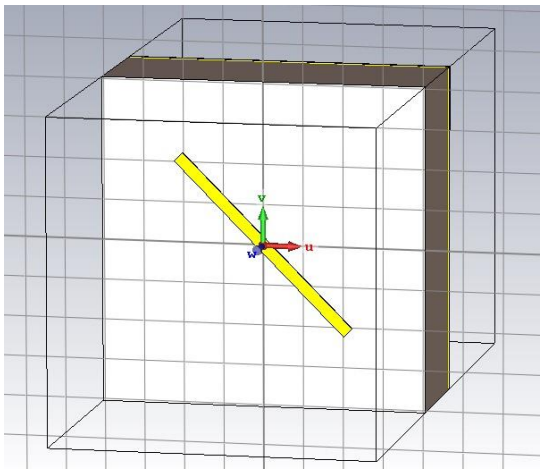

Fig: Part 2(cut-wire resonator)

```
clc;
close all;
clear;
A=readmatrix('PART1S11.txt');
B=readmatrix('PART1S12.txt');
C=readmatrix('PART2S11.txt');
D=readmatrix('PART2S12.txt');
freq=A( :,1);
part_A_S11=A( :,2);
part_A_S12=B( :,2);
part_B_S11=C( :,2);
part_B_S12=D( :,2);

plot(freq,part_A_S11,'k')
hold on;
plot(freq,part_A_S12,'r')
hold on;
plot(freq,part_B_S11,'m')
hold on;
plot(freq,part_B_S12,'c')
hold on;
xlabel('frequency');
ylabel('Reflection(in dB)');
grid on;
title('Reflection vs Frequency');
```

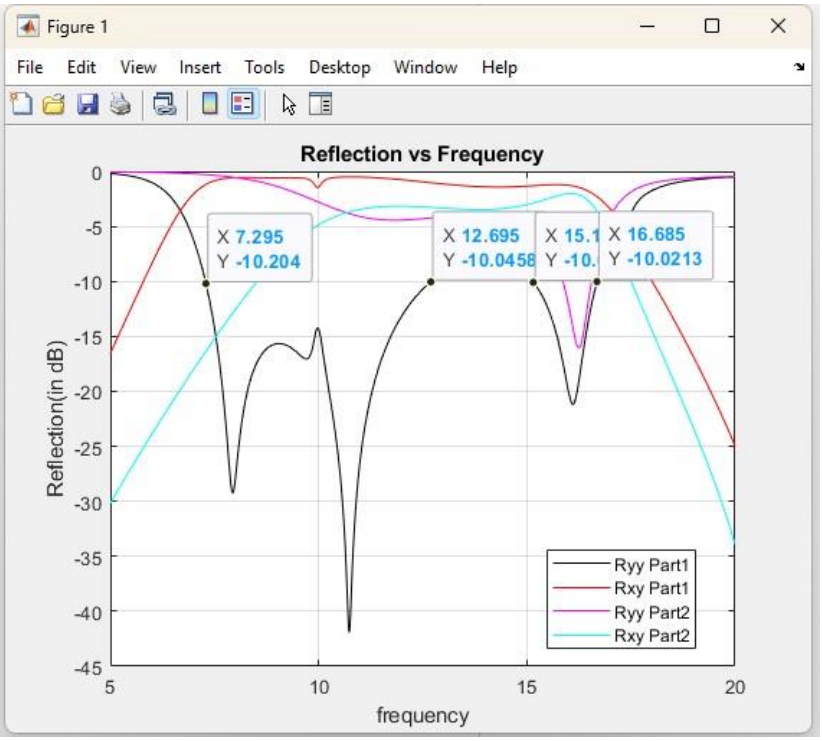

Fig 5(a): Co- and cross-polarized reflection coefficients.

Figure 5 illustrates the co- and cross-polarized reflection coefficients as well as the Polarization Conversion Ratio (PCR) for parts I and II. Part I exhibits co-polarization (ryy) consistently below -10 dB from 7.295 to 12.695 GHz and 15.155 to 16.685 GHz, accompanied by a PCR exceeding 0.9 within the range of 7.415 to 12.47 GHz and 15.41 to 16.61GHz. The observed frequency difference between the co-polarization and PCR bandwidths is primarily attributed to dielectric losses. Notably, three resonance frequencies at 8.045, 10.775, and 16.175 GHz demonstrate nearly 100% polarization conversion. Regarding part II, it is evident that it contributes less to polarization conversion in the lower band but significantly more in the higher band. Part II achieves a PCR surpassing 0.8 from 15.725 to 16.595 GHz, with a peak value occurring at 16.235 GHz, demonstrating almost 100% polarization conversion.

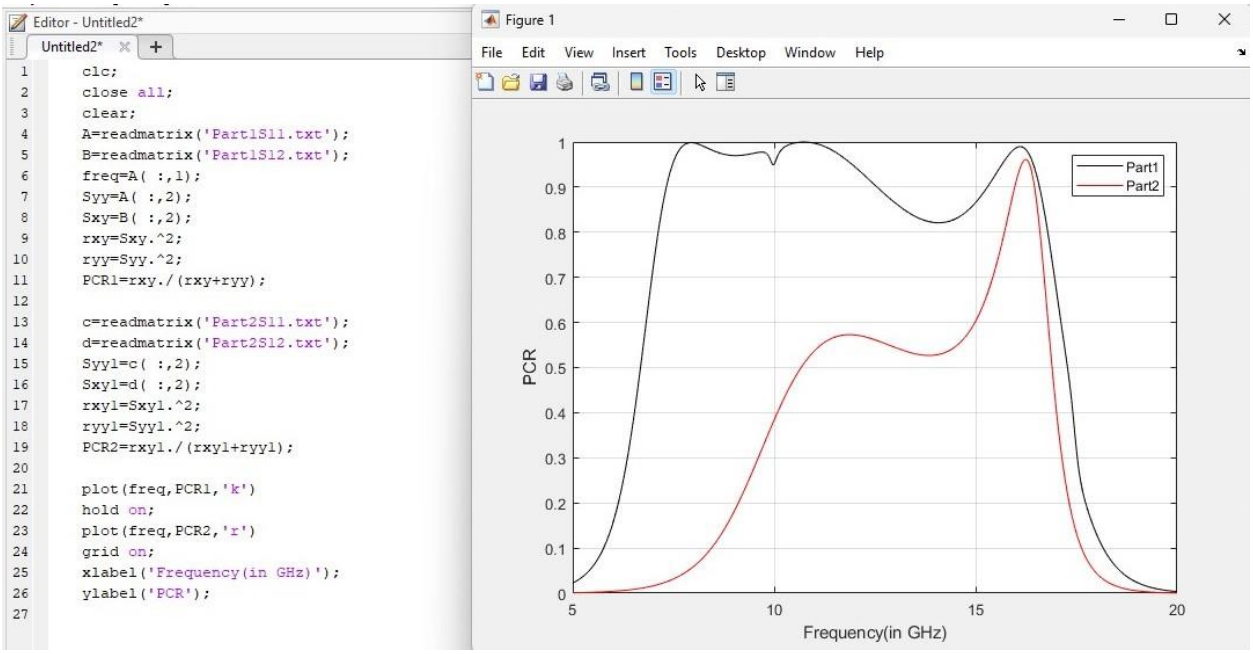

Fig 5(b): PCR versus Frequency

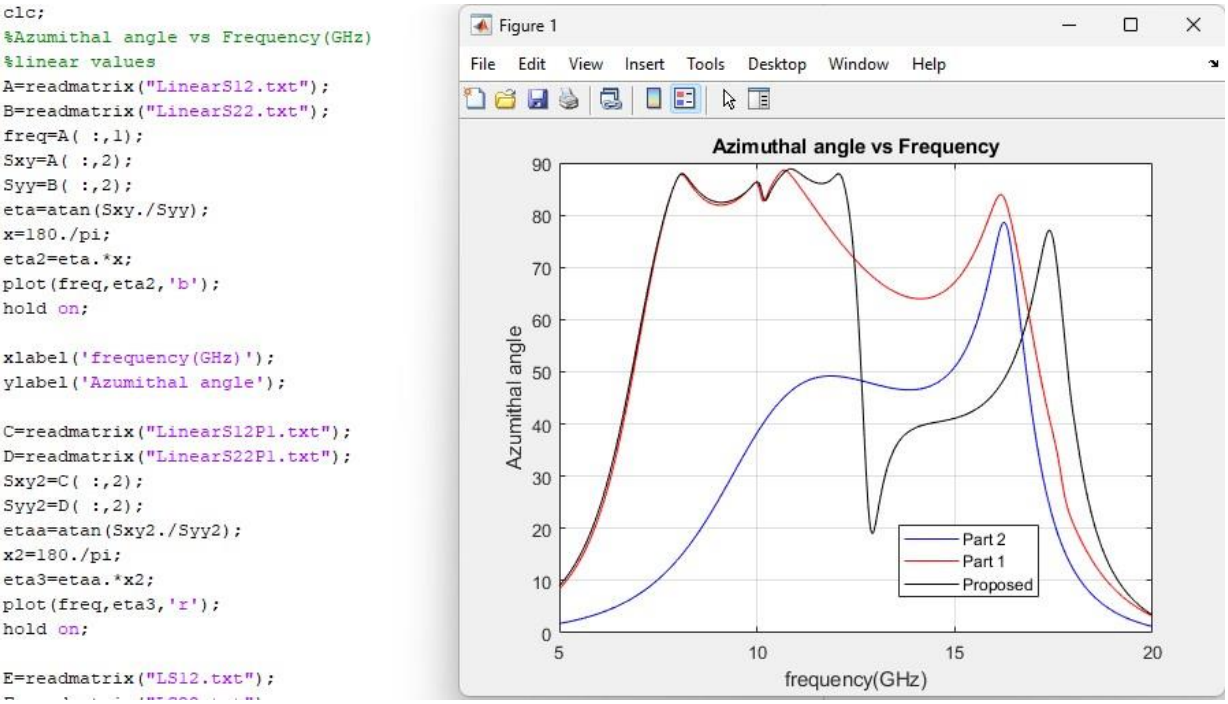

Fig 6(a): Azimuthal angle (η)

```
clc;
clear ;
A=readmatrix('DBS22.txt');
B=readmatrix('DBS12.txt');
C=readmatrix('DBS22P1.txt');
D=readmatrix('DBS12P1.txt');
E=readmatrix('AR_S11.txt');
F=readmatrix('AR_S12.txt');
freq=A( :,1);
txx=A( :,2);
tyy=B( :,2);
txx2=C( :,2);
tyy2=D( :,2);
freq2=E( :,1);
txx3=E( :,2);
tyy3=F( :,2);
deltaphixy=45;
a=(txx.^4)+(tyy.^4)+(2.*(txx.^2).*(tyy.^2).*cos(2.*deltaphixy));
x=(txx.^2)+(tyy.^2)+sqrt(a);
y=(txx.^2)+(tyy.^2)-sqrt(a);
q=x/y;
AR1=sqrt(q);
AR=20*log(AR1);
plot(freq,AR,'k')
hold on;
a2=(txx2.^4)+(tyy2.^4)+(2.*(txx2.^2).*(tyy2.^2).*cos(2.*deltaphixy));
x2=(txx2.^2)+(tyy2.^2)+sqrt(a2);
y2=(txx2.^2)+(tyy2.^2)-sqrt(a2);
```

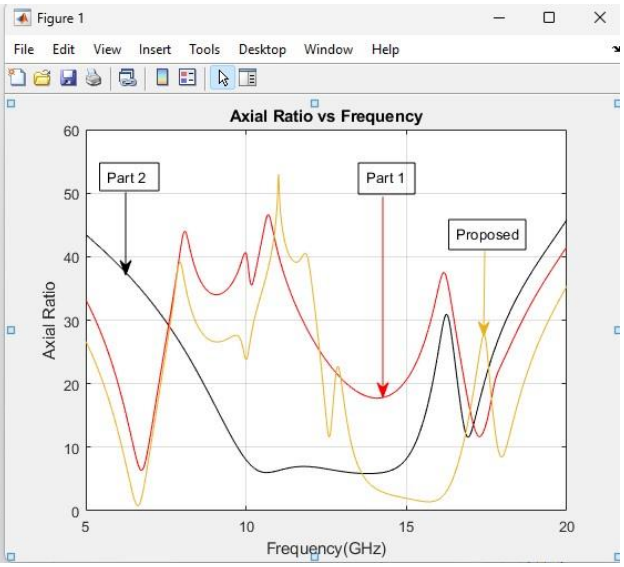

Fig 6(b): AR versus Frequency

Furthermore, Fig. 6 provides information on the azimuth angle, phase difference between the total reflected fields along the x- and y-axes, and the Axial Ratio (AR) of the reflection wave. As depicted in Fig. 6(a), there is notable consistency in the azimuth angle between part I and the proposed structure within the lower frequency band (5–12 GHz). This observation affirms that part II has minimal impact at lower frequencies. However, in the higher frequency band, the curve of the proposed structure descends rapidly and then stabilizes at an angle of $\eta = 45^\circ$, diverging from the behavior of part I. This is attributed to the influence of part II, which primarily operates in the higher frequency range. Fig. 6(b) illustrates the AR values across the frequency range for parts I, II, and the proposed structure. It is evident that the reflected electromagnetic wave's polarization state, when converted by parts I and II, is either linear or elliptical. In contrast, the proposed structure transforms the reflected electromagnetic wave into linear polarization in the lower band and circular polarization in the higher band.

Conclusion:

A wideband and high-efficiency reflective polarization converter based on meta surface is suggested in this report to convert the LP incident EM into orthogonal LP reflection waves in the lower band and CP reflection waves in the higher band. The simulation findings show that it achieves greater than 0.88 PCR for a linear-to-linear polarization conversion from 7 to 12.3 GHz. Furthermore, a fractional bandwidth of 13.0% from 14.7 to 15.62 GHz can be obtained for a linear-to-circular polarization conversion. The experimental results agree reasonably well with the simulations. Because of its linear-to-linear and linear-to-circular polarization conversion capabilities, the suggested design has potential applications in polarization-manipulation devices and antenna design.